Advances in Intelligent Systems Research, volume 165
International Conference on Modeling, Simulation, Optimization and Numerical Techniques (SMONT 2019)

Modeling and Simulation of Millimeter Wave Radiation Detection for Buried Metal Targets

Qi Zhang, Guangfeng Zhang *, Changchang Yu, Yuan Gao, Li Zhu and Hong Wang
School of Electronic Engineering and Optical Technology, Nanjing University of Science and Technology, Nanjing 210094, China
*Corresponding author

***Abstract*—Due to the high penetration of the millimeter wave, some hidden metal and non-metallic objects can be detected effectively. So millimeter wave plays an important role in the military and has been widely used in many fields such as guidance, communication, radar, radiation measurement and remote sensing. However, in the shallow covert detection, the research of millimeter wave radiation is rarely involved. Based on this, with the passive radiation characteristics and antenna temperature contrast theory of metal target analyzed, this paper starts from the millimeter wave radiation modeling of metal targets. Through sampling point-by-point, the simulation and imaging of metal targets which are buried under sand are also discussed. The experimental results show that the millimeter wave can penetrate the thin sand layer, detect the target and image, which provides theoretical and experimental support for the application of millimeter wave used in shallow-buried detection and lay the foundation for further research.**

Keywords—millimeter wave; radiation characteristic; shallow-buried metal; radiation image; simulation

I. INTRODUCTION

Compared with visible light and infrared, the millimeter wave is less restricted of weather conditions. When the target is detected, working all-weather and all-day, the millimeter wave radiometer has higher precision and stronger penetration[1]. The passive millimeter wave(PMMW) detection system has good performance for the detection of metal targets, which makes it attract much attention. Just as radar technology can be used in many fields to detect through common concealment, PMMW technology has certain application potential in the detection and imaging of concealed targets. In related theoretical research, Chen Wei, Cao Dongren and others modeled the millimeter wave radiation characteristics of metal spheres[2], but did not image specifically; Yuan Long, Yin Ming et al. proposed a method to detect the metal target based on millimeter-wave radiometer imaging[3], but their research is in lack of the analysis of the target in the image; Liu Jing et al. explored the radiation of solid targets such as metal spheres and cylinder theoretically and experimentally. They analyzed and summarized the radiation characteristics and differences of different three-dimensional structures[4], but the shallow-buried metal was not studied. Based on this, in this letter, with the passive radiation characteristics and antenna temperature contrast theory of metal target analyzed, the radiation of planar metal was modelled. At the same time, we did a simulation from which we get the PMMW radiometric image of metal targets which are shallow- buried. Finally, some analyses were presented as well.

II. DICKE RADIOMETER

The system block diagram of the Dicke radiometer is show n in Figure 1[5]. The switch is add so that the input signal of th e receiver can be modulated to alternate periodically between t he antenna and the comparative noise source (reference sourc e). Synchronous detectors, switch drivers and square wave gen erators are also inset to ensure that the frequency of detectiona nd switching are the same. In order to keep the system gain G constant for one cycle to eliminate its effects, the rate of the in put switch f_s needs to be adjusted to be higher than the maxim um spectral component in the gain fluctuation[6].

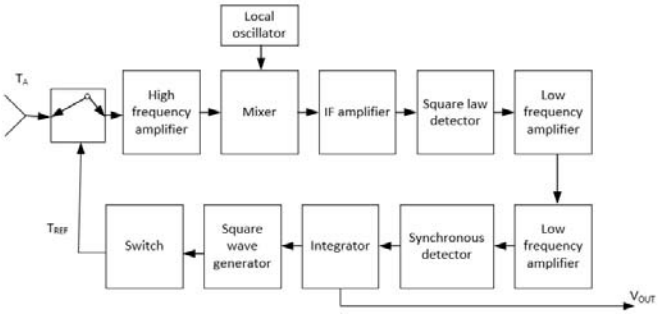

FIGURE I. DICKE RADIOMETER SYSTEM BLOCK DIAGRAM

The measurement uncertainty due to system gain variation ΔT_G is,

$$\Delta T_G = \left(T_{REF} - T_A'\right)\frac{\Delta G}{G} \tag{1}$$

T_{REF} ——the equivalent noise tempera ture of the reference load;

T_A' —— the input noise temperature of the antenna;

τ_s —— switching cycle;

The measurement uncertainty caused by input signal noise $T_{REF} + T_{REC}'$ during half of the integration time of the reference load is,

$$\Delta T_{NREF} = \frac{T_{REF} + T'_{REC}}{\sqrt{B\tau/2}} = \frac{\sqrt{2}(T_{REF} + T'_{REC})}{\sqrt{B\tau}} \quad (2)$$

The measurement uncertainty caused by noise temperature $T_A' + T'_{REC}$ during half of the time the antenna is turned on is,

$$\Delta T_{NANT} = \frac{\sqrt{2}(T_A' + T'_{REC})}{\sqrt{B\tau}} \quad (3)$$

Generally, under unbalanced conditions, according to (1), (2) and (3), $\Delta T_{\min}$ is as follows,

$$\begin{aligned}\Delta T_{\min} &= \left[\left(\Delta T_G\right)^2 + \left(\Delta T_{NREF}\right)^2 + \left(\Delta T_{NANT}\right)^2 \right]^{\frac{1}{2}} \\ &= \left[\frac{2(T_{REF} + T'_{REC})^2 + 2(T_A' + T'_{REC})^2}{B\tau} + \left(\frac{\Delta G}{G}\right)^2 \left(T_{REF} - T_A'\right)^2 \right]^{\frac{1}{2}}\end{aligned} \quad (4)$$

If the load temperature T_c is controllable, ΔT_G can be suppressed through $T_{REF} = T_A'$.At this time, the influence of gain on the sensitivity of the system is eliminated, and the system can be considered to be in equilibrium. The sensitivity is,

$$\Delta T_{\min} = \frac{2(T_A' + T'_{REC})}{\sqrt{B\tau}} = \frac{2T_{sys}}{\sqrt{B\tau}} \quad (5)$$

III. METAL TARGET MODELLING

As shown in Figure 2, there is a metal plane on the ground. Its area is A_T, which can be represented by coordinates as $A_T = (x_2 - x_1)(y_2 - y_1)$. At a high position for H, a radiometer is used to detect the target at an angle of θ_F, AS is the antenna beam centerline. The radiation characteristics of metal planar targets are modelled in two cases:

A. The Area of Antenna Beam is Bigger than the Target

Let the stereo beam angle of the main beam of the radiometer antenna be Ω_M, the angle of the solid target to the antenna is Ω_T, Considering the high main beam efficiency of the antenna and ignoring the influence of its side lobes, the antenna temperature can be expressed as,

$$\begin{aligned}T(\theta_F) &\simeq \frac{1}{4\pi}\int_{\Omega_M} T_{AP}(\theta,\phi)G(\theta,\phi)d\Omega \\ &= \frac{1}{4\pi}\left[\int_{\Omega_T} T_{APT}(\theta,\phi)G(\theta,\phi)d\Omega + \int_{\Omega_M - \Omega_T} T_{APB}(\theta,\phi)G(\theta,\phi)\right]d\Omega\end{aligned} \quad (6)$$

In (6), $G(\theta,\phi)$ is the antenna gain, $T_{APT}(\theta,\phi)$ is the apparent temperature of the target, $T_{APB}(\theta,\phi)$ is the background apparent temperature.

If there is no metal target, the temperature of antenna is,

$$T(\theta_F) = \frac{1}{4\pi}\int_{\Omega_M} T_{APB}(\theta,\phi)G(\theta,\phi)d\Omega \quad (7)$$

The expression of the antenna temperature contrast can be obtained by subtracting the two types,

$$\Delta T_A(\theta_F) = \frac{1}{4\pi}\int_{\Omega_T} [T_{APT}(\theta,\phi) - T_{APB}(\theta,\phi)]G(\theta,\phi)d\Omega \quad (8)$$

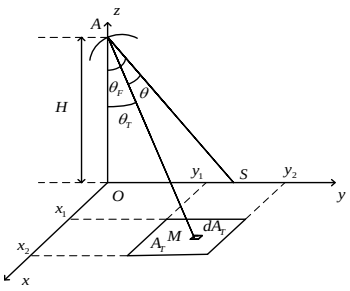

FIGURE II. METAL PLANE TARGET DETECTION MODELING DIAGRAM

To simplify the calculation, it is assumed that the center of the metal plane target is located at the center of the beam of the observation antenna. When the observation height is large, the angle of the target to the antenna θ_T is small[7], so the equation(8) can be further written as,

$$\begin{aligned}\Delta T_A(\theta_F) &= \frac{1}{4\pi}\Delta T_{AP}(\theta_F)\int_{\Omega_T} G_0 e^{-b\theta^2} d\Omega \\ &= \frac{G_0}{4b}\Delta T_{AP}(\theta_F)(1 - e^{-bA_T\cos^3\theta_F / \pi h^2})\end{aligned} \quad (9)$$

In conclusion, if A_T/h^2 remains unchanged, ΔT_A will not change as well. Therefore, it is possible to simulate the measurement of the real target under high altitude conditions by controlling A_T/h^2 constant. This similar scaling analog measurement brings great convenience to actual engineering exploration [8].

B. The Area of Antenna Beam is Smaller than the Target

At this point, the resulting formula is similar to (9), where A_T becomes the projected area of the antenna beam on the target.

IV. SIMULATION RESULTS AND ANALYSIS

Because the imaging target of the study is static, the imaging rate can be not too fast. In order to obtain sufficient integration time for better imaging results, we simulate and image by sampling point-to-point. The antenna beam center meshes the imaging area to collect radiation data and ensures sufficient scanning time.

The experimental conditions are as follows: We use the 8m

m Dicke radiometer system with a Cassegrain antenna. Grid ma pping was used to get enough integration time. The interval is a bout half of the main beam width to ensure the image Quality. The test height is about 70cm. 8mm band radiometer parameter s are shown in Table 1.

TABLE I. PARAMETERS OF 8MM RADIOMETER SYSTEM

Parameters	**8mm**
Center frequency /GHz	35
Beamwidth / °	8
Band-width / GHz	2
Mixer noise figure /dB	4
Integration time /s	1
Sensitivity /K	0.2

The experiment was sited in Dongpuzi, Nanjing. The temperature of the day was 30 °C, cloudy. The rectangular metal frame target was buried in the sand and imaged by the above-mentioned detection equipment. The experimental environment scene is shown in Figure 3:

FIGURE III. EXPERIMENT ENVIRONMENT

The external imaging scene are shown in Figure 4, where Figure 4(a) is the target to be tested: a metal frame with a built-in rectangle, which is buried in the sand during imaging, and the scene is shown in Figure 4 (b).

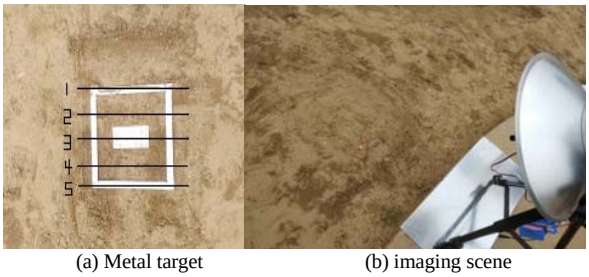

(a) Metal target (b) imaging scene

FIGURE IV. OUTFIELD OF SHALLOW-BURIED METAL TARGET IMAGING

Through simulation, by sampling according to 5 line segments like Figure 4(a), the radiation characteristic of mantal target is shown as Figure 5.

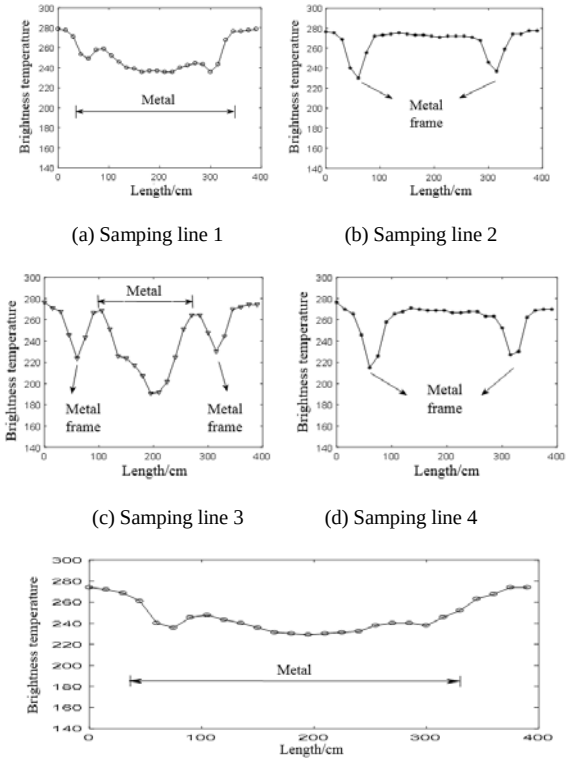

(a) Samping line 1 (b) Samping line 2

(c) Samping line 3 (d) Samping line 4

(f) Samping line 5

FIGURE V. RADIATION CHARACTERISTIC OF MANTAL TARGET

The grayscale image and pseudo-color image obtained in the experiment are shown in Figure 6. For the convenience of observation and processing, the original grayscale image is reversed without affecting the further processing results of the later image. The result is Figure 6 (b).

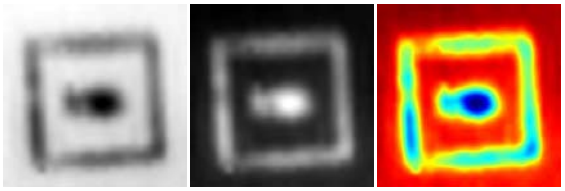

(a) Grayscale (b) Grayscale inversion (c) Pseudo color image

FIGURE VI. MILLIMETER WAVE RADIATION IMAGE OF SHALLOW-BURIED METAL IN EXTERNAL FIELD

This experiment is the first attempt, and the thickness of the fine sand laid is small. According to the imaging results, the millimeter wave can penetrate the thin fine sand, and the target is detected and imaged effectively. During the experiment, it was found that the humidity and thickness of the sand have a great influence on the imaging results of the buried metal targets, especially the humidity.

V. CONCLUSION

This paper carried out the modeling, simulation and imaging of shallow-buried metal targets. Firstly, the principle of Dicke radiometer was introduced. Then, the metal radiation modeling was conducted to show the characteristic of metal. On this basis, the 8mm radiometer was used to simulate and image the metal target buried in the sand. The experimental results show that the millimeter wave can penetrate the thin fine sand, detect the target and image. In contrast, millimeter waves have a good balance between penetration and imaging resolution, and thus they have unique advantages in the detection of hidden objects. However, due to the complex external environment and many interference factors, the specific influence of the thickness and humidity of fine sand on the real time imaging of shallow-buried metal targets needs further study and analysis.

ACKNOWLEDGMENT

We gratefully acknowledge the financial support of National Natural Science Foundation (grant number 61371038) and Jiangsu Overseas Research & Training Program for University Prominent Young & Middle-aged Teachers and Presidents.

REFERENCES

[1] Li Beibei, Zhang Guangfeng, Lou Guowei. Water surface vegetation detection method based on millimeter wave radiation characteristics[J].Computer Measurement & Control,2016,24(7):45-48.

[2] CHEN Wei, CAO Dong-ren, WU Li, et al. Modeling and analysis of millimeter wave radiation characteristics of metal spheres[J]. Optoelectronic Engineering, 2013, 40(4).

[3] Yuan Long, Yin Ming, Yin Zhongke, et al. Detection of metal targets by millimeter wave radiometer [J]. Laser and infrared, 2006, 36(10):1004-1006.

[4] Liu J, Zhang G, Zhou L. Study on MMW radiation characteristics and imaging of stereoscopic metal targets[C]. Society of Photo-optical Instrumentation Engineers. Society of Photo-Optical Instrumentation Engineers (SPIE) Conference Series, 2016.

[5] Zhang Guangfeng, Zhang Zuyin, Guo Wei. Index Measurement and Imaging Experiment of Absolute Value Detection Dick Radiometer[J]. Telemetry and Remote Control, 2003, 24(6):30-34.

[6] Gui Liangqi, Zhang Zuyin, Guo Wei. A review of improving the sensitivity of microwave radiometers[J]. Telemetry and Remote Control,2004, 25(6):1-5.

[7] Shi Xiang. Passive millimeter wave detection and its stealth technology research [D]. Nanjing University of Science and Technology, 2008.

[8] Zhang Zuyin, Lin Shijie. Microwave radiation measurement technology and application [M]. Electronic Industry Press, 1995